

# Detection and Location of Partial Discharges in Power Transformers using Acoustic and Electromagnetic Signals

**Sacha M. Markalous**

LDIC GmbH  
 Zschoner Ring 9  
 Kesselsdorf, 01723, Germany

**Stefan Tenbohlen and Kurt Feser**

Stuttgart University  
 Pfaffenwaldring 57  
 70569 Stuttgart, Germany

## ABSTRACT

The measurement of partial discharges (PD) is a non-destructive and sensitive diagnostic tool for the condition assessment of insulating systems. Two major tasks of PD measurements may be distinguished, (i) PD detection, hence providing evidence and the type of the PD and (ii) the location of the PD. The question “Where is the PD source?” is amongst others tremendously important for scheduling and starting maintenance/repair actions cost and time efficiently or to perform a risk analysis. Here the possibility to geometrically localize the flaw, by means of arrival times of acoustic PD signals, gets an extremely interesting option. Precise acoustic arrival times are consequently essential to accurately locate PD in a power transformer. The averaging of acoustic PD signals helps to enhance the acoustic sensitivity. The acoustic detection limit is lowered significantly and the determination of the arrival times is made possible for weaker PD. Supplementary steps, like automatic objective arrival time determination or additional wavelet-based de-noising further improve the overall location accuracy. A new location approach works with pseudo-times and allows for the use of robust direct solvers instead of the previously used iterative algorithms.

Index Terms — PD location, electromagnetic (UHF) and acoustic PD measurements, de-noising, wavelet, acoustic averaging, arrival time determination.

## 1 INTRODUCTION

THE insulating system of a power transformer is a major part and its integrity has a decisive role for the safe operation of the unit. Assessments and diagnosis of the insulation condition are hence necessary. Weaknesses of the insulating systems may lead to a predisposition of failures triggered from external stresses such as short circuits, lightning strokes or transients of switching operations. Information about the insulation characteristics form extensive fundamentals for conditioned-based maintenance approaches, serve as asset appraisements, support continuous risk assessment and can also help in the early detection of failures.

The well-known and approved diagnostic examination of partial discharges (PD) is regarded a powerful, non-

destructive and sensitive diagnostic tool for the condition assessment of insulating systems. For the instant diagnostic examination of PD within oil-paper insulated transformers basically three different physical signals directly related to the PD are currently used: (i) electric signals, (ii) acoustic signals and (iii) electro-magnetic signals.

## 2 ACOUSTIC AND ELECTROMAGNETIC PD DETECTION

PD in oil cause, in addition to the measurable electrical pulses, acoustic waves in the ultra-sonic range (20 kHz – 1 MHz) [1, 2] and electromagnetic waves up to the UHF range (0.3 – 3 GHz) [3-5]. Performed on-site/on-line electric PD measurements on transformers according to the IEC 60270 standard show certain drawbacks and limitations. In contrast electromagnetic (UHF) and acoustic PD measuring methods have advantages for on-site/on-line applications.

Their sensors can be applied on-line and a high immunity against certain external disturbing signals is given. An additional benefit is the inherent possibility of a three dimensional determination of the failure location using acoustic PD arrival times [5].

For the acoustic PD measurements piezoelectric sensors mounted on the outside of the transformer are used. The sound velocity in oil for operational temperatures between 50° C and 80° C may e.g. vary from around 1240 m/s to 1300 m/s [6]. Basically, insulation materials feature a low-pass character [7] and the acoustic attenuation increases with good approximation proportional to the square of the frequency  $f^2$  [8].

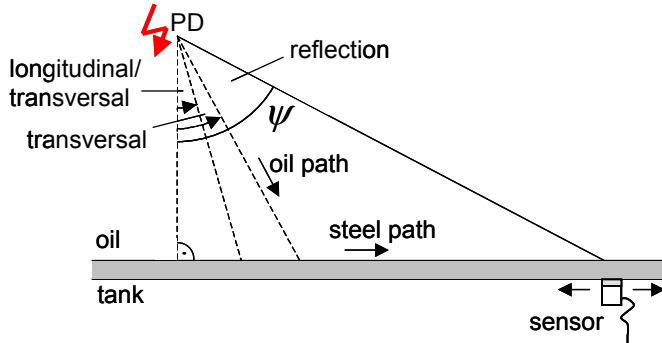


Figure 1. Illustration of the structure-borne path problem: acoustic sensor is not directly located normal to the PD source hence the propagation path has portions of oil (simplified comprising oil, possibly pressboard and winding parts as well) and steel.

Figure 1 illustrates the so-called structure-borne path problem. It can cause early readings of the acoustic arrival times. The mechanical waves hitting the housing create an alternative propagation path via the tank wall with larger wave speeds than in oil. Using arrival times of signals, travelled partly on the structure-borne path in combination with an average sound velocity valid merely for oil, would imply an incorrect distance between source and sensor [9].

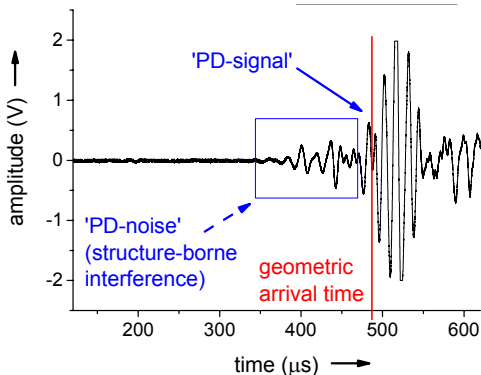


Figure 2. Acoustic PD signal (apparent charge of 491 pC) with highlighted known arrival time and preceding structure-borne interferences.

Systematic investigations of this matter were carried out [10, 11]. An acoustic sensor was gradually moved on a steel plate from a position perpendicular to an acoustic source in oil, to positions involving a growing portion of a metal plate (Figure 1). Depending on the angle  $\Psi$  three regions can be distinguished where different wave types are predominantly stimulated. For PD location using an

average sound velocity mainly geared to the propagation speed in oil only signal portions of the direct way should be denoted as 'PD-signal' [5]. Structure-borne interferences can be addressed as 'PD-noise' instead (see UHF-triggered acoustic PD signal in Figure 2). In Figure 2 additionally to the acoustic and electromagnetic UHF PD measurements simultaneous electric PD measurements (according to the IEC 60270 standard) were performed giving readings in Picocoulomb for comparisons (this was also done in measurements presented in the following chapters).

### 3 MATHEMATICS OF SPATIAL PD LOCATION USING ACOUSTIC ARRIVAL TIMES

Regarding the PD location two main approaches can be found: (i) on the one hand alterations of the signal amplitude or deformations of the signals shape along the propagation path can give hints for a source location, (ii) on the other hand measured arrival times are used to calculate the origin of signals (often referred to as “triangulation”).

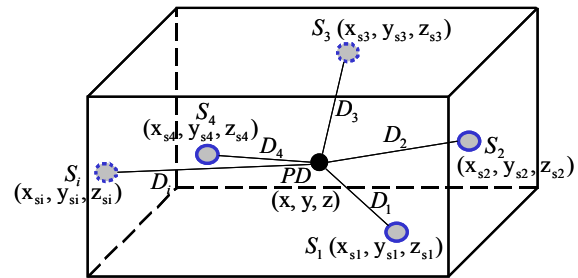


Figure 3. External acoustic sensors on a transformer tank with a PD inside using Cartesian coordinates.

Figure 3 shows a schematic view of a transformer tank with  $i$  attached acoustic sensors, PD inside and the resulting distances  $D_i$  from the sensors  $S_i$  to the PD origin. Such arrangements are the geometric basis for the involved mathematical formulations. The appropriate nonlinear observation equations are in the simplest case characterized by sphere functions which intersect at the PD origin.

Depending on whether mixed-acoustic (i.e. triggering with the electric or electromagnetic PD signal) or all-acoustic measurements are used the number of unknowns is three (space coordinates  $(x, y, z)$  of the PD) or four (an additionally unknown temporal origin) respectively. Hence an exact spatial location of the PD origin needs in the determined case at least three or four usable acoustic arrival times in the sensor signals.

A new approach within the acoustic signal processing works with pseudo-times and allows the usage of robust direct Global Positioning System (GPS) solvers instead of the previously used iterative algorithms [12].

#### 3.1 ABSOLUTE TIME APPROACH

For mixed acoustic measurements, i.e. use of a triggering with an electric or an electromagnetic PD signal, the instant the PD occurs is known. Mathematically this corresponds to an absolute time measurement, illustrated in Figure 4.

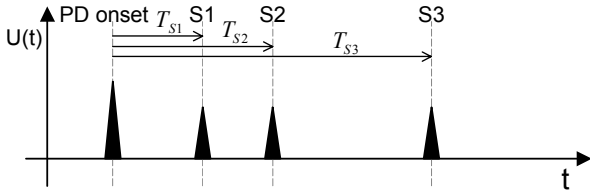


**Figure 4.** Schematic visualization of acoustic arrival times in reference to the known PD onset (electric/electromagnetic PD trigger signal).

The associated sphere functions with the three unknown PD coordinates in space  $(x, y, z)$ , the measured arrival times  $T_{Si}$ , the assumed sound velocity  $v_s$  and the cartesian sensor coordinates  $(x_{si}, y_{si}, z_{si})$  have the following appearance

$$(x - x_{s1})^2 + (y - y_{s1})^2 + (z - z_{s1})^2 = (v_s \cdot T_{S1})^2 \quad (1),$$

$$(x - x_{s2})^2 + (y - y_{s2})^2 + (z - z_{s2})^2 = (v_s \cdot T_{S2})^2 \quad (2),$$

$$(x - x_{s3})^2 + (y - y_{s3})^2 + (z - z_{s3})^2 = (v_s \cdot T_{S3})^2 \quad (3).$$

These are functions describing spheres with radii  $D_i$  which are defined with

$$D_i^2 = (v_s \cdot T_{Si})^2 \quad (4)$$

The approximation of a vanishing propagation delay of e.g. the electromagnetic PD signal (nanosecond range) is valid because the acoustic signals show typical delay times in the range of micro- up to millisecond range.

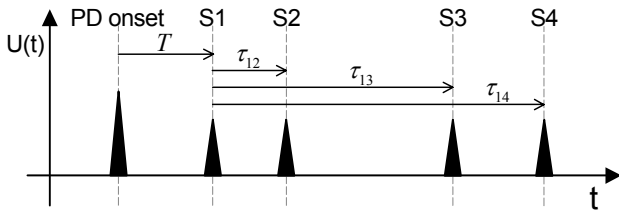


**Figure 5.** Schematic visualization of the acoustic time differences  $\tau_{li}$  in reference to the unknown PD onset represented by the additional temporal fourth unknown  $T$ .

### 3.2 TIME-DIFFERENCES APPROACH

For all-acoustic PD measurements the exact instant the PD occurs is unknown (no electric/UHF signal trigger used). The acoustic sensor which is first hit triggers a recording process on all sensors simultaneously. Not being over-determined for four acoustic signals, results in three time-differences  $\tau_{li}$  starting from the first-hit reference sensor (Figure 5). Compared to the equations (1 - 3), just the right hand sides (4) of the sphere functions are modified with an additional temporal unknown  $T$  and the measured time-differences  $\tau_{li}$  [5, 12]. From a geometrical point of view, the PD site is defined as the intersection point of rotation-symmetric hyperboloids.

### 3.3 PSEUDO-TIME APPROACH

A new alternative of stating the system of non-linear observation equations uses pseudo-times  $T'_{Si}$ . This results in a “GPS (Global Positioning System) mode” of the formulas, since all-acoustic measurements with four or more sensors act like an “inverse” satellite-receiver positioning problem and result hence in mathematically

related formulas. In this case the auxiliary unknown is a “receiver” time offset  $\Delta t$ . Figure 6 depicts how the pseudo-times of four acoustic signals are connected to the unknown PD onset.

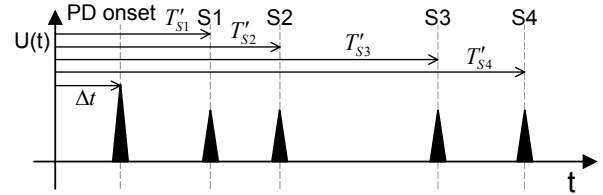


**Figure 6.** Schematic visualization of acoustic pseudo-times in reference to the unknown PD onset.

The observation equations become symmetric due to the fact that the unknown time offset  $\Delta t$  is contained in all pseudo-times  $T_{Si}$ . The pseudo-time notation turned out to be very universal for acoustic source location since it even allows localizing defects with absolute time information from mixed-acoustic measurements [5]. In terms of pseudo-times this is the special case of a vanishing time offset  $\Delta t$ . Other fields of mechanical location problems as quantitative sound emission analysis [13] and earthquake location [14] can also be handled with this approach.

### 3.4 ALGORITHMIC SOLUTION STRATEGIES

Non-linear equation systems (e.g. (1 - 3)) are commonly solved with iterative algorithms. One great drawback of these solvers is the sometimes strong dependency on the initial value (which must be provided from the user). The solutions of all the presented location approaches could be computed iteratively. Nevertheless a great advantage of the pseudo-time notation is a utilization of direct solution strategies available for GPS-problems. They exist for the determined [15] and also for the over-determined case [16]. With the use of direct algorithms one gets rid of the initial value dependency. Furthermore the direct solver featured much more stable results in the presence of inevitable measuring errors, sensitivity limits or wrongly assumed acoustic propagation velocities [12].

## 4 SIGNAL PROCESSING

Basic signal processing steps for the acoustic PD location procedure are (i) signal de-noising and (ii) subsequent arrival time determination. The general feasibility of the positioning depends on the correct objective arrival time determination, which is synonymous in determining the true beginning of a transient signal.

For de-noising of acoustic PD signals averaging (UHF-triggered or acoustic-triggered) should be performed. Further de-noising can be achieved wavelet-based. This enables better results in the following arrival time determination.

### 4.1 OBJECTIVE ARRIVAL TIME DETERMINATION

Two alternatives of arrival time determination can be generally distinguished – manual time determination

(performed by an experienced analyst) or automatic time picking. Simple threshold triggering can be used, although high errors in the resulting arrival time information might be introduced. More sophisticated techniques might be classified into criteria which detect changes in either the (i) energy of the signal or the (ii) frequency content of the signal.

#### 4.1.1 ENERGY CRITERION

The energy criterion is based on the observation that sound emission signals, in particular when of middle to bad quality, are predominantly characterised by a variation of their energy content, rather than a fluctuation of their frequency composition [17]. The energy curve  $S_i$  of the sampled signal  $x$  is here defined as a cumulative sum of amplitude values. The separation of the signal from the noise part and the realization of the criterion are managed with

$$S'_i = S_i - i\delta = \sum_{k=0}^i (x_k^2 - i\delta) \quad (5)$$

where a negative trend  $\delta$  is introduced ( $i$  is the loop variable, ranging through all samples of a selected part of a signal). The trend is dependent on the total energy of the signal  $S_N$  and the signal length  $N$  (with  $N$  the number of samples). It is determined by

$$\delta = \frac{S_N}{\alpha \cdot N} \quad (6)$$

The calculated partial energy curve features a global minimum which, so the assumption, corresponds with the signals arrival time or onset respectively (Figure 7). The slight systematic delay, mentioned and corrected in [17] by means of a factor  $\alpha > 1$  in (6), has not been considered in this contribution, the factor was always chosen to  $\alpha = 1$  for simplicity.

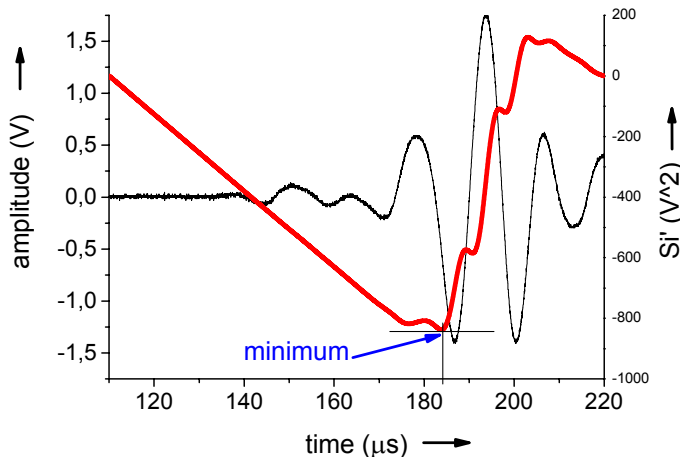


Figure 7. Acoustic signal (thin line) with its partial signal energy curve (bold line) exhibiting a minimum.

#### 4.1.2 AKAIKE INFORMATION CRITERION (AIC)

Auto-regressive (AR) time picking techniques are founded on the assumption that seismograms or acoustic emissions respectively, can be divided into locally stationary segments - before and after the onset of the

signal - with two different auto-regressive processes modelling them. Either the order of the AR process or the values of the auto-regressive coefficients - or both - change, as the characteristics of the consecutive segments are altered.

The Akaike Information Criterion (AIC) normally gives indications about the quality or the order of an AR process fitting a time series. It was shown that the AIC function can be calculated directly from the sampled signal  $x$  of length  $N$  [13, 18]. The estimated onset of the signal coincides with the global minimum of the computed AIC value. The results for both picking algorithms are compared in the case studies following in chapter 5.

#### 4.2 DE-NOISING OF ACOUSTIC PD SIGNALS USING AVERAGING

Increasing the signal-noise-ratio by suppressing noise contained in signals with averaging is a very effective method implying some prerequisites: (i) the signals are repetitive, (ii) signal and noise are uncorrelated and (iii) the noise is supposed to be white (white noise should feature a fairly constant spectral density in the frequency range investigated). During an averaging process, the noise included in the signals tends towards its statistic mean value, which is zero, if white noise is assumed. The repetitive part of the signal is superimposed constructively and remains unaffected. The theoretical maximum signal-noise-ratio gain is  $N^{0.5}$  where  $N$  is the number of superpositions [9, 19].

To be successful with acoustic averaging a stable trigger of a physical signal related to the PD with a higher sensitivity than the acoustic ones is required. Such a combination of two PD signals of different type and sensitivity is classically used in test laboratories of transformer manufacturers, where the sensitive electric PD signal is combined with the acoustic signals to locate PD. The same holds for an UHF acoustic combination since comparative investigation on the sensitivity revealed a higher UHF sensitivity especially for hidden defects [20]. The previously resulting acoustic sensitivity can be enhanced, as well on-line.

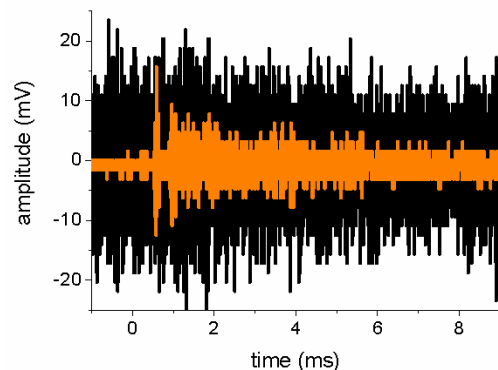


Figure 8. Comparison of an acoustic 132 pC single PD pulse (black line) and 500 superpositions of maximum 9 pC (orange line) from the same experimental arrangement.



In Figure 8 a comparison of an acoustic PD single pulse signal with an apparent charge of 132 pC and an UHF-triggered averaged acoustic PD signal with 500 superpositions of maximum 9 pC is presented in the same scale (Picocoulomb values known from simultaneous electric PD measurements according to IEC 60270). Although both signals were recorded within the same experimental arrangement (identical PD source, sensor and sensor position and an equal signal amplification), the single acoustic PD pulse showed no clearly observable information. However, the averaged acoustic PD signal with 500 superpositions features an obviously visible pulse. The UHF PD signals, which triggered the averaging process, were detectable for discharges with apparent charges down to 5 pC. Regarding the experimental arrangement, it was tried to model realistic acoustic circumstances. For that purpose, the configuration involved a disc-winding package at high voltage surrounded by two pressboard cylinders with a stimulated PD at the inner side, immersed in an oil-filled transformer tank (Figure 11).

#### 4.3 WAVELET DE-NOISING OF ACOUSTIC PD SIGNALS

Cases may arise, where the PD might fluctuate strongly in their intensity or fade rapidly before the de-noising, introduced through the averaging process, has reached a satisfactory level. Wavelet-based de-noising provides an alternative to further enhance the signal-noise-ratio. Another application would be the improvement of non-averaged acoustic single pulse measurements.

##### 4.3.1 'STANDARD' WAVELET DE-NOISING

Basic steps of the wavelet-based de-noising comprise transformation into the wavelet space, thresholding of coefficients and back transformation. The back transformation results in an estimation of the unknown signal (of which the noisy version was measured) ideally with reduced noise content.

Without going into details in [21] a threshold  $\tau$  was given, which cancels most of the coefficients caused by the noise (with standard deviation  $\sigma$ ), while at the same time leaving the significant signal coefficients unchanged

$$\tau = K \cdot \sqrt{2 \cdot \ln(N)} \cdot \sigma \quad (7)$$

The threshold is conditioned by the number of coefficients  $N$  and a constant  $K$ , can be introduced. The included generally unknown standard deviation  $\sigma$  of the noise is estimated. Regarding the wavelet family the Daubechies wavelet family (wavelets db2 – db7) fits best to the acoustic PD signals analyzed, whereof the wavelet db5 was used most of the time. Cases, in which the above mentioned constant  $K$  was chosen to one, are considered as 'standard' de-noising [5].

**Table 1.** Different degrees of an UHF-triggered acoustic averaging PD measurement.

No. of superpos	Original averaged		De-noised averaged	
	energy	AIC	energy crit.	AIC
2500	300.0 $\mu$ s	288.2 $\mu$ s	300.4 $\mu$ s	263.8 $\mu$ s
1000	300.8 $\mu$ s	288.2 $\mu$ s	300.6 $\mu$ s	263.2 $\mu$ s
200	436.0 $\mu$ s	420.2 $\mu$ s	300.1 $\mu$ s	285.4 $\mu$ s

Arrival time information obtained with the energy and AIC criterion (the geometric arrival time was  $t = 298.5 \mu$ s, wrong time picks are highlighted); Wavelet De-Noising constant  $K=1$ .

In Table 1 experimental results are given for further wavelet-based de-noising (constant  $K = 1$ ) on already averaged signals. The averaged signals with a high number of superpositions (1000 and 2500) featured an already sufficient signal-noise-ratio. Both used arrival time criteria managed to obtain a reasonable estimate of the known geometrical arrival time of  $t = 298.5 \mu$ s. For lower signal-noise-ratios, here 200 superpositions, the arrival time determination with the energy criterion and the AIC failed, resulting in a far too late time picking. In contrast, after the wavelet-based de-noising, both criteria gave reasonable results again.

##### 4.3.2 'EXCESSIVE' WAVELET DE-NOISING

In cases the de-noising constant  $K$  is chosen greater than one the "smoothness" of the original signal might not be retained and the expectancy of the mean-squared error of the signal estimation might rise. Regardless of the integrity of the original signal, tests with a greater constant  $K$  were carried out, resulting in reconstructed acoustic time signals like in Figure 9.

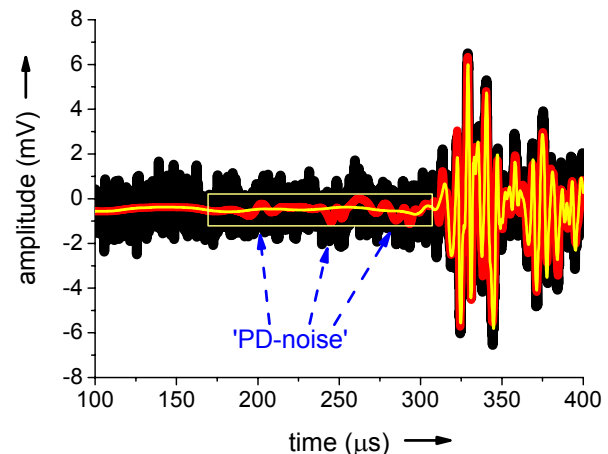


**Figure 9.** Original averaged signal with 20 superpositions (bold dark line), de-noised signals with  $K=1$  (bold light line, 'PD-noise' is highlighted with a thin line rectangle) and de-noised signals with  $K=2$  (thin line).

Figure 9 gives the original averaged signal and two wavelet-based de-noised signals ( $K = 1$  and  $K = 2$ ). Assuming the oscillations in the de-noised signal with the constant  $K = 1$  (highlighted with a thin line rectangle) are due to 'PD-noise' (structure-borne pulse, compare chapter 2.2), the further de-noising with the constant  $K = 2$  lead to a removal of them.

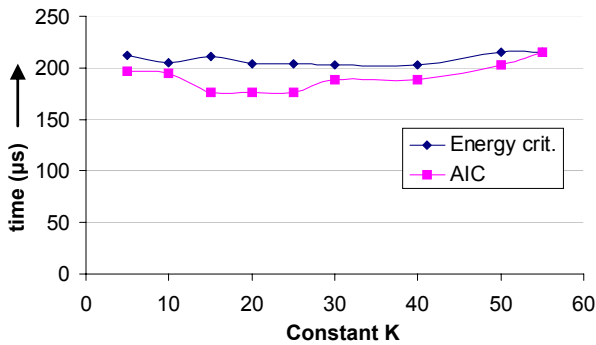


Figure 10. Arrival time investigation using the energy criterion and the AIC on an acoustic 575 pC single pulse with strongly varying constant  $K$  (the geometric arrival time was  $t = 220.95 \mu\text{s}$ ).

Encouraged by these kinds of results, the arrival time information of a UHF-triggered acoustic single pulse of a 575 pC PD was analyzed with the energy criterion and the AIC. The PD pulse had a geometric arrival time of  $t = 220.95 \mu\text{s}$  and the investigation was conducted with strongly varying de-noising constant  $K$ . In Figure 10, the computed arrival times for several different values of the constant  $K$  are given. The AIC again yielded early pickings, while the energy criterion matched better. The arrival times approached for higher  $K$  factors, reaching finally for  $K = 55$   $t = 215.47 \mu\text{s}$  for the energy criterion and  $t = 214.97 \mu\text{s}$  for the AIC respectively.

## 5 CASE STUDIES OF PD LOCATIONS

### 5.1 LABORATORY MEASUREMENTS

The experimental configuration of UHF-triggered acoustic PD measurements with ad hoc visible acoustic PD single pulses of 575 pC PD and initially noise-covered maximum 9 pC is shown in Figure 11. It contains a disc winding package at high voltage, surrounded by two pressboard cylinders, with a stimulated PD, at the inner side of the coil, immersed in an oil-filled transformer tank [22]. The transformer housing was situated in a high voltage laboratory and had dimensions of 1.77 m x 0.77 m x 1.56 m.

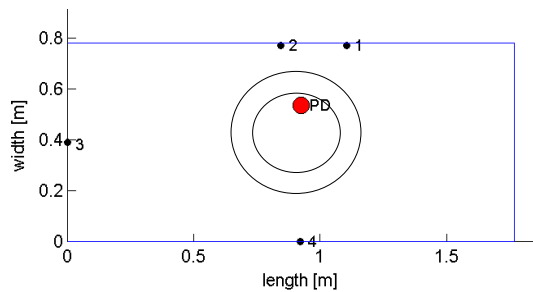


Figure 11. Top view of the arrangement of four acoustic sensors on the transformer tank with a PD inside the disc winding package.

The UHF sensor was inserted through a standardized oil valve and its signals were detected unamplified. On the outside of the tank four piezo-electric acoustic sensors and 60 dB amplifiers were attached to capture the acoustic PD signals. The UHF measurements used a transient recorder

with an analogue bandwidth of 3 GHz which triggered the acoustic transient recorder with an analogue bandwidth of 200 MHz performing the acoustic averaging. A simultaneous electric PD measurement according to IEC 60270 was carried out.

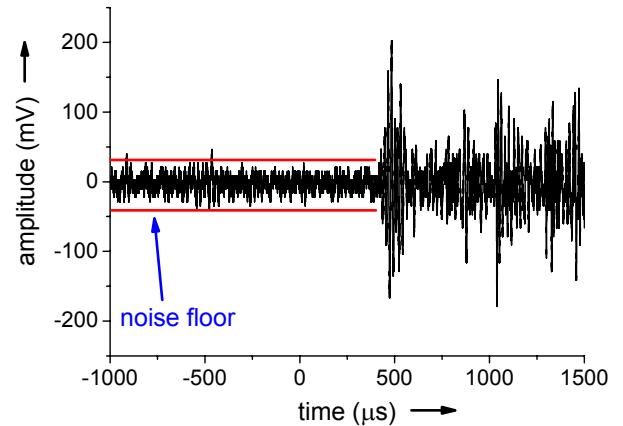


Figure 12. Acoustic single pulse of a 575 pC PD (maximum impulse amplitude 202.5 mV, noise floor approximately 30 – 45 mV, highlighted with two solid lines) of sensor 2.

The acoustic single pulse detection limit is around 100 - 130 pC in the experiment. PD at the inner side of the winding was stimulated with an electrode on ground. The apparent charges of the PD were varied from several pC to several hundreds of pC. The oil temperature in the tank was 21 °C and the corresponding sound velocity used for the location calculations 1417 m/s.

Figure 12 pictures the acoustic 575 pC PD signal of sensor 2 with a noise floor of approximately 30 – 45 mV. The signals of the other channels had a very similar appearance. In the corresponding maximum 9 pC averaged acoustic signal of 500 superpositions at sensor 2 the noise floor has been diminished to approximately 3.2 mV during the averaging process and the maximum positive pulse amplitude was 12.5 mV. This averaged pulse is completely hidden in the noise floor of the single pulse measurement.

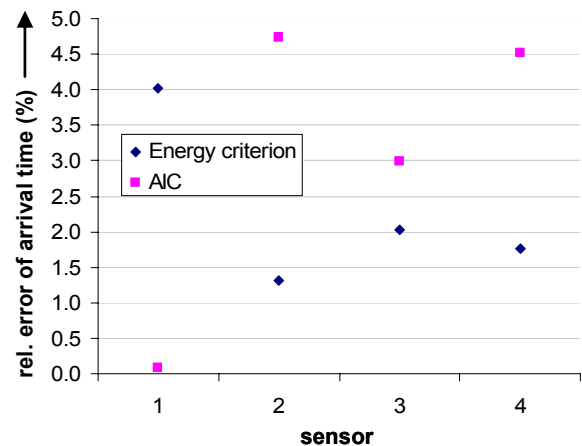
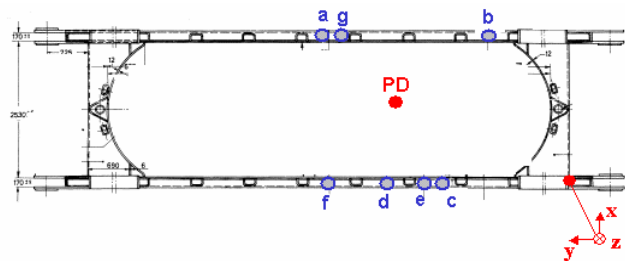


Figure 13. Comparison of the relative error of acoustic arrival times of the 575 pC measurement obtained with the energy criterion and the AIC, respectively, for the four acoustic sensors.

The determined arrival time information for the 575 pC measurement is compared for the energy and AIC criteria in Figure 13 for the four acoustic sensor signals. These relative arrival time errors result in a mean relative error of 2.3 % for the energy criterion and of 3.1 % for the AIC for the 575 pC measurement. The mean relative error of arrival times for the 9 pC averaged measurements (not shown) were higher, reaching 6.5 % and 9.5 % for the energy criterion and AIC respectively. Using the automatically determined energy criterion arrival times, the pseudo-times approach and the direct solver [16] the location results for the 575 pC measurement featured a spatial deviation of 2.8 cm and 12.1 cm for the 9 pC averaged measurement.



**Figure 14.** Top view of the housing of the 200 MVA transformer with attached acoustic sensors and the calculated PD location inside.

## 5.2 ON-SITE MEASUREMENTS

Over a period of several months on- and off-line all-acoustic PD measurements were performed on-site at a 200 MVA single-phase transformer, whose gas-in-oil diagnosis indicated PD. During an off-line applied voltage test an electrical PD measurement revealed PD with apparent charges up to 600 pC and with an acoustic PD measurement (referred to as 'measurement 1') acoustic pulses were recorded on four sensors simultaneously [5]. Figure 14 pictures the top view of the housing of the transformer with the sensor positions and the calculated PD location.

In Table 2 the location results are summarized. The result of 'measurement 1' was determined with an iterative solution algorithm. The remaining two measurements the direct solver for over-determined systems was used [16]. The arrival times were calculated with the energy criterion. Through the fact that in 'measurement 2' and 'measurement 3' the estimated PD site of independent measurements remained almost the same (spatial deviation of 5.4 cm) a certain reliability of the results was achieved. As well the spatial deviation between the results of the off-line 'measurement 1' and the on-line 'measurements 2/3' using different sensor positions, different number of sensors and also different average sound velocities (based on the different oil temperatures) is in a rather reasonable range. The spatial deviation between 'measurement 1' and 'measurement 2' is 17.0 cm, while it is 18.2 cm between 'measurement 1' and 'measurement 3'.

## 6 CONCLUSION

As diagnostic tool PD measurements are with an increasing degree a distinct means of the condition assessment or the

asset management of aged devices. To get a comprehensive PD diagnostic for transformers on-line/on-site, it is helpful or even necessary to complement electric PD measurements with acoustic and electromagnetic measurements (UHF range).

For the estimation of the PD site precise measurements of acoustic arrival times and robust positioning algorithms are essential. Based on experiences made in experimental and practical measurements a collection of important steps for acoustic PD location on transformers has been gathered (supplementing information in [9]). This 'modus operandi' touches the following main aspects:

- (i) Reasonable sensor placement [9]:  
placing sensors where they can vibrate as free as possible.
- (ii) Mixed-acoustic PD measurements:  
if possible acoustic signal/noise-ratio should be improved through averaging.
- (iii) Post-processing of measured signals:  
wavelet-based de-noising and objective arrival time criteria deliver reliable results.
- (iv) Solving the PD location problem:  
Estimate resulting acoustic propagation velocity (use mean oil temperature and corresponding sound velocity as good guess), iterative solution algorithms or new direct one-step solvers can be used for the calculational solution.

**Table 2.** Location results of acoustic PD measurements over a period of several months with changing sensor positions (compare sensor positions a, ..., g in Figure 6).

Calculated PD-origin	x [m]	y [m]	z [m]
measurement 1 (off-line a, b, c, d)	1.40	3.12	2.27
measurement 2 (on-line c, d, e, f, g)	1.25	3.19	2.23
measurement 3 (on-line a, c, d, e, f, g)	1.27	3.22	2.19

These results regarding the improvement of acoustic PD measurements and signal processing steps characterize requirements for acoustic PD detection and location systems. Acoustic transient recorders should in view of the de-noising effect of signal averaging support this function. PD location software on the other hand might include features for objective arrival time determination and wavelet-based de-noising of the acoustic PD signals.

## REFERENCES

- [1] R. T. Harrold, "Ultrasonic Spectrum Signatures of Under-Oil Corona Sources", IEEE Trans. Electr. Insul., Vol. 10, pp. 109-112, 1975.
- [2] E. Howells and E. T. Norton, "Detection Of Partial Discharges In Transformers Using Acoustic Emission Techniques", IEEE Trans. Power Apparatus Syst., Vol. 97, pp. 1538-1546, 1978.
- [3] W. R. Rutgers and Y. H. Fu, "UHF PD-Detection in a Power Transformer", 10th Intern. Sympos. High Voltage Engineering, Québec, Canada, pp. 219-222, 1997.

[4] M. D. Judd, B. M. Pryor, S. C. Kelly and B. F. Hampton, "Transformer Monitoring Using the UHF Technique", 11th Intern. Sympos. High Voltage Engineering, London, UK, pp. 362-365, 1999.

[5] S. M. Markalous, Detection and Location of Partial Discharges in Power Transformers using Acoustic and Electromagnetic Signals, Ph.D. thesis, University of Stuttgart, Germany, 2006.

[6] E. Howells and E. T. Norton, "Parameters affecting the velocity of sound in oil", IEEE Trans. Power Apparatus Syst., Vol. 103, May pp. 1111-1115, 1984.

[7] M. Beyer, H. Borsi and M. Hartje, "Some aspects about possibilities and limitations of acoustic Partial Discharge (PD) measurements in insulating fluids", 5th Intern. Sympos. High Voltage Engineering, Braunschweig, Germany, pp. 1-4, 1987.

[8] E. Grossmann, "Akustische Teilentladungsmessung zur Überwachung und Diagnose von Öl/Papier-isolierten Hochspannungsgeräten", Dissertation, University of Stuttgart, Germany, 2002.

[9] Partial Discharge Tests in Transformers Working Group of Transformers Committee, "Draft Guide for the Detection and Location of Acoustic Emissions from Partial Discharges in Oil-Immersed Power Transformers and reactors", IEEE PC57.127/D1.1 Standards Draft 3, 2003.

[10] L. E. Lundgaard, W. Hansen and K. Dursun, "Location of discharges in power transformers using external acoustic sensors", 6th Intern. Sympos. High Voltage Engineering, New Orleans, USA, Vol. 1, Paper No. 15.05, pp. 1-4, 1989.

[11] B. T. Phung, R. E. James, T. R. Blackburn and Q. Su, "Partial discharge ultrasonic wave propagation in steel transformer tanks", 7th Intern. Sympos. High Voltage Engineering, Dresden, Vol. 7, Paper No. 74.04, pp. 131-134, 1991.

[12] S. M. Markalous, S. Tenbohlen and K. Feser, "New robust non-iterative algorithms for acoustic PD-localization in oil/paper-insulated transformers", 14<sup>th</sup> Intern. Sympos. High Voltage Engineering, Beijing, China, Paper No. G40, 2005.

[13] J. H. Kurz, "Verifikation von Bruchprozessen bei gleichzeitiger Automatisierung der Schallemissionsanalyse an Stahl- und Stahlfaserbeton", Dissertation, University of Stuttgart, 2006.

[14] J. H. Kurz, S. M. Markalous, C. U. Grosse and H.-W. Reinhardt, "New approaches for three dimensional source location - examples from acoustic emission analysis", European Geosciences Union - General Assembly, Vienna, Austria, Geophysical Research Abstracts, Vol. 7, 06373, 2005.

[15] L. O. Krause, "A Direct Solution of GPS-Type Navigation Equations", IEEE Trans. Aerospace and Electronic Systems Vol. 23, pp. 225-232, 1987.

[16] S. Bancroft, "An algebraic solution of the GPS Equations", IEEE Trans. Aerospace and Electronic Geodactica, Vol. 21, pp. 56-59, 1985.

[17] C. U. Grosse and H. Reinhardt, "Schallemissionsquellen automatisch lokalisieren - Entwicklung eines Algorithmus", MP Materialprüfung, Carl Hanser Verlag, München, Germany, Vol. 41, pp. 342-347, 1999.

[18] H. Zhang, C. Thurber and C. Rowe, "Automatic P-wave arrival detection and picking with multiscale wavelet analysis for single-component recording", Bulletin of the Seismological Society of America, Vol. 93, pp. 1904 - 1912, 2003.

[19] E. Howells and E. T. Norton, "Location of Partial Discharge sites in on-line transformers", IEEE Trans. Power Apparatus Syst., Vol. 100, pp. 158-161, 1981.

[20] R. Kuppaswamy and T. Floribert, "Comparative Investigations on UHF and Acoustic PD Detection Sensitivity in Transformers", IEEE Intern. Sympos. Electr. Insul. (ISEI), Boston, Massachusetts, USA, pp. 150 - 153, 2002.

[21] D. L. Donoho, "De-noising by soft-thresholding", IEEE Trans. Information Theory, Vol. 41, pp. 613 - 627, 1995.

[22] S. M. Markalous, S. Tenbohlen and K. Feser, "Improvement of acoustic detection and localization accuracy by sensitive electromagnetic PD measurements under oil in the UHF range", 14<sup>th</sup> Intern. Sympos. High Voltage Engineering, Beijing, China, Paper No. G39, 2005.



**Sacha M. Markalous** (M'07) received the Dipl.-Ing. degree in electrical engineering from the University of Stuttgart, Germany, in 2002. In 2006 he received the doctorate degree at the Institute of Power Transmission and High Voltage Technology, University of Stuttgart in the field of Ultra-High Frequency Partial Discharge measurement and acoustic location in power transformers. In 2006 he joined LDIC GmbH, Dresden, Germany as technical director where he is coordinating the departments of product research & development, product management, service activities and production. Here his work comprises diagnostics, monitoring and high-voltage measurement techniques of power cables/accessories, transformers, gas-insulated systems and overhead-lines. Dr.-Ing. Markalous contributed to more than 40 papers. He is member of the German Power Engineering Society VDE-ETG.



**Stefan Tenbohlen** (M'07) received the Diploma and Dr.-Ing. degrees from the Technical University of Aachen, Germany, in 1992 and 1997, respectively. In 1997 he joined AREVA Schorch Transformatoren GmbH, Mönchengladbach, Germany, where he was responsible for basic research and product development and in this function worked in the field of on-line monitoring of power transformers. From 2002 to 2004 he was the head of the electrical and mechanical design department. In 2004 he was appointed to a professorship and head of the institute of Power Transmission and High Voltage Technology of the University of Stuttgart, Germany. In this position his main research fields are diagnostic of equipment of electrical networks, development of high voltage measurement technique, behavior of gas insulated insulation systems and different aspects of electromagnetic compatibility (EMC). Prof. Tenbohlen holds several patents and has published more than 100 papers. He is member of the German committees of CIGRE A2 (Power Transformers), D1 (Emerging Technologies), C4 (System Technical Performance) and several international working groups. Since 2007 he has been a member of the board of the German Power Engineering Society VDE-ETG.



**Kurt Feser** (F'89) was born in Garmisch-Partenkirchen, Germany, in 1938. He received the Dip.-Ing. and Dr.-Ing. degrees from the University of Munich, Munich, Germany, in 1963 and 1970, respectively. In 1971, he joined Haefely and Cie AG, Basel, Switzerland, as a Chief Development Engineer. Since 1980, he has been Director and Member of the executive board of Haefely, responsible for capacitors and high-voltage test equipment. In 1982, he joined the University of Stuttgart, Stuttgart, Germany, as Head of the Power Transmission and High Voltage Institute. He retired in 2004. Prof. Feser is a member of VDE and CIGRE and former chairman of IEC TC 42 "High Voltage Test Technique" and the author of many papers.